

Prediction of tool wear based cutting forces during end milling of Inconel 718 using artificial neural networks

Agata Felusiak-Czyryca^{1*} , Paweł Twardowski¹ 

¹ Faculty of Mechanical Engineering, Poznan University of Technology, ul. Piotrowo 3, 60-965 Poznan, Poland

* Corresponding author's e-mail: agata.felusiak-czyryca@put.poznan.pl

ABSTRACT

During the research, correlation between the input parameters (cutting parameters and cutting forces measure like peak to peak, root mean square and root mean square of ripple) and the variables were searched for, and the sensitivity of the network to input parameters was determined. In this paper artificial neural networks (ANNs) to prediction of tool wear based on cutting forces were used. Multilayer perceptron (MLP) networks with backward error propagation were used. The research shows that for the tested material and in the tested range, the cutting parameters are not diagnostically significant for the prediction of VB_c (band width of the corner wear). The authors of this article focus on simplifying the model and analyzing the influence of variables on the prediction error. Neural networks show a correlation of about 95% for test sets.

Keywords: Inconel 718, machining, cutting forces, tool wear prediction, artificial neural network.

INTRODUCTION

Large industries such as aviation and automotive require frequent use of materials with special properties, usually require high resistance to corrosion, high strength and good machinability. Assumptions about the strength of corrosion resistance and the preservation of properties at high temperatures are met by nickel-based alloys.

Machining of these alloys is difficult due to the high temperature occurrence in the cutting zone, outer-metal chip notch formed on the edge, the elastic recovery of the machined layer and hardening of the material during machining. For this reason, it is difficult to predict the value of tool wear [1]. Inconel machining causes significant changes in the microstructure of the processed material [2–5]. In the paper [2] the authors compared the microstructure and stress in the surface layer of turned Inconel 718 with PCBN and ceramic inserts. In all tested cases, plastic deformation and heat generation in the cutting process caused clear microstructural changes. The Grain fragmentation under the influence of strong

plastic deformation was observed. Depth profiles of the tested specimens showed residual stresses with surface tension and subsurface compression due to local plastic deformation and heating.

Xavior et al. [4] investigated the effect of machining under different cutting conditions with different tool materials on microstructure, residual stress and work hardening of Inconel 718. The authors noticed that during dry machining tensile stresses raised significant on the treated surface and greater grain degradation occurred than during machining with cooling. On the other hand, when flood cooling was used, the greater microhardness occurred. When machining nickel-based alloys, there is a strong adhesion between the tool and the workpiece, which affects tool wear, roughness and forces. By increasing the speed, the temperature in the cutting zone rises, which leads to the hardness increase of the workpiece and results in an escalation cutting forces [5]. The forces also increase with increasing other cutting parameters (depth, feed). However, these mechanisms are typical for machining resulting for machining when the cutting layer cross-section

growth and consequently of cutting force increases. In the article [6], cryogenic cooling with liquid nitrogen was used which significantly reduced the temperature in the cutting zone and improve lubrication, what resulted reduction of the occurrence of adhesion phenomena and grain degradation. The roughness value Ra was lowered by 88%. The condition of the cutting edge has a significant influence on the roughness of the machined surface. In the article [7] authors studied surface integrity and fatigue in the end milling of Inconel 718. They used tools with three tool flank wear levels: 0, 0.1, 0.2. Under these conditions they found that higher tool wear produced less surface roughness. However, in the article [8] the authors analyzed a wider range of cutting insert wear. They proved that during the break-in of the tool, the roughness was high. Depending on the tool geometry it decreased or remained constant. The roughness subsequently increased when tool wear overcome $VB = 0.3\text{--}0.4$ mm.

Taking into account the properties of Inconel indicated in the literature and the significance of the impact of tool wear on the quality of the manufactured elements and the difficulties in predicting wear during machining, the authors decided to use artificial neural networks in research. ANNs are most often used to predict or monitor the condition of the edge [9–12] or the roughness of the machined surface in machining [13,14]. In paper [15], the authors used artificial neural networks to predict tool wear during Inconel 718 turning on the basis of variable cutting speed and cutting time. In their research, the prediction error was different depending on the cutting speed. NN training and testing was carried out by the “leave-k-out” method, which is particularly useful when dealing with small training sets. Received RSME error 0.005–0.038. In the article [16], the prediction errors of the tool wear value for regression analysis and artificial neural networks for Inconel turning were compared, showing more than twice as high error in the case of regression. Similar conclusions were reached by the authors [17], who milled Inconel

718 in their research, and used cutting parameters and corner radius as input parameters. Researchers in [18] show a higher usefulness of the genetic algorithm than ANN for predicting the maximum wear on the flank surface. A strategy based on ANN for estimating tool flank wear is presented in [19]. The ANN-based system was trained using real-time RMS signals of cutting force and torque (M_z) from the three axes (F_x, F_y, F_z), cutting and time parameters. Showing a total error of 5.42%. In paper [20], the authors use neural networks to predict tool wear during steel turning. As input parameters, using data from many sensors, e.g. forces, temperatures and vibrations and demonstrate the validity of the measurements used. The authors [21] used the values of force amplitudes in the frequency and time domains to predict tool wear using neural networks.

The authors of this article use force measures in the time domain and cutting parameters to predict tool wear. In addition, they determine the measures and parameters most suited to the prediction of the tool condition. In many publications, the authors do not focus on the validity of the input parameters used in the construction of models, and often use only one measure (e.g. RMS) for the recorded variable, which may omit significant predictor variables.

MATERIALS AND METHODS

Tests were carried out on an Inconel 718 workpiece. Mass fractions of elements in Inconel 718 are shown in Table 1. A four-edge carbide milling cutter (P8700450 by Fraisa) dedicated to machining nickel-based alloys was used. The tool diameter was 10 mm and the cutting length was 50 mm. The five identical tools were used. The research was carried out on vertical machining center DMC 70V hi-dyn (DMG Mori).

The end milling operation was carried out according to cutting parameters and cutting plan (a_p – cutting depth, v_c – cutting velocity, a_e – cutting

Table 1. Mass fractions of elements in Inconel 718 alloy

Percentages	Ni	Cr	Nb	Mo	Ti	Al	Co	Si
Min. %	50	17	4.75	2.8	0.65	0.2	-	-
Max.%	55	21	5.50	3.30	1.15	0.80	1.00	0.35
Percentages	Mn	Cu	C	P	S	B	Fe	
Min. %	-	-	-	-	-	-	-	
Max.%	0.35	0.30	0.08	0.015	0.015	0.006	Balance	

width, f_z – feed per tooth) presented in Table 2. Five-level central composite experimental design was used. Full data on the cutting parameters in each pass and the value of tool wear and cutting time are contained in Table 3. Table 3 does not take into account repeated passes.

Figure 1 shows a simplified scheme of measurement path used during the tests. The following are the technical parameters of the measurement and measuring instruments. Forces were measured in three directions by three-directions piezoelectric dynamometer (own design). The sensitivity of the dynamometer are for x-axis 8.6 pC/N, y-axis 8.7 pC/N, z-axis 3.4 pC/N and natural frequency $f_n = 8$ kHz. The signal from the dynamometer was transmitted to the Kistler charge amplifier type 5015 A. The measuring range was ± 2000 N and the built-in low pass filter was set to 30 kHz. Then the signal was sent to the analog-to-digital A/D converter with the sampling frequency $f_s = 6000$ Hz for each channel. From the A/D converter, the signals were transferred to a computer and digitally processed using special software. Based on time signals, time-domain measures were determined: root mean square (RMS), peak to peak (P-P), ripple RMS (ripple). In the following, these measures were used as inputs to the neural network.

In this paper RMS values of cutting forces were analyzed. This allows among others to avoid

differences in signs resulting from the sense of a force vector. The RMS value was given by the formula (1), peak to peak formula (2) and ripple RMS formula (3).

$$RMS = \sqrt{\frac{1}{T_2 - T_1} \int_{T_1}^{T_2} [x(t)]^2 dt} \quad (1)$$

$$P - P = P_{\max \text{ high}} + P_{\max \text{ low}} \quad (2)$$

$$RIPPLE_RMS = \sqrt{\frac{1}{T_2 - T_1} \int_{T_1}^{T_2} [x(t) - K]^2 dt} \quad (3)$$

where: RMS – root mean square, K – the constant component of the shift.

The time period T used in the calculations was 2 s. Tool wear parameters were measured after each pass in the same spot on the corner. Wear parameter and VB_c (band width of the corner wear) for each edge were measured. After each measurement, the arithmetic mean for the four corners was calculated. Tool wear was measured using a workshop microscope with a measurement accuracy of 0.01 mm. The measured value is shown in Figure 2. The wear was photographed using the Zeiss Stereo Discovery V.20 microscope. In the further part of the article, the average value of tool wear for four corners was assumed.

Artificial neural networks of the MLP (multi-layer perceptron) type with backward error propagation, with one hidden layer and one output

Table 2. Cutting parameters

Parameters	Program levels				
	-2	-1	0	1	2
v_c [m/min]	15	25	30	35	40
a_p [mm]	1	3.5	6	9	12
a_e [mm]	0.1	0.3	0.5	0.75	1
f_z [mm/tooth]	0.02	0.025	0.030	0.035	0.040

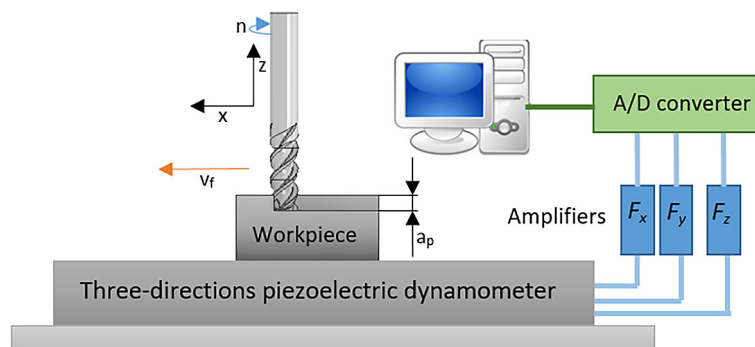


Figure 1. Scheme of measurement path used during the tests

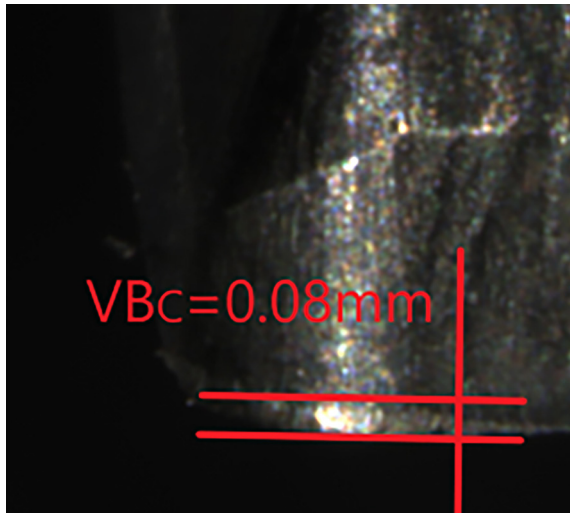


Figure 2. Tool wear: $VB_c = 0.08$ mm, $v_c = 25$ m/min, $v_f = 107$ mm/min, $a_p = 9$ mm, $a_e = 0.75$ mm. magnification x48

neuron were used in the research. During the tests, various sets of input variables were used, which included cutting parameters (v_c, v_f, a_e, a_p), cutting time t_c , RMS values of cutting forces ($F_{i_{RMS}}$), RMS values of ripple ($F_{i_{ripple}}$) and values peak to peak ($F_{i_{p-p}}$). All measures were measured in three directions, f – in the direction of the feed, z – in the direction of the z axis and fN - normal to the feed direction.

RESULTS AND DISCUSSION

Full data on the cutting parameters in each pass and the value of tool wear and cutting time are contained in Table 3. Table 3 does not take into account repeated passes. Based on the results presented in Table 3, the tool wear results in all passes with repetitions shown on Figure 3. Statistica software was used in further analyses.

Subsequent points on the graph do not have constant cutting parameters, so it is not a wear curve. Due to the use of different cutting parameters, it is not possible to establish a direct relationship between wear and cutting time.

None of the determined measures show a direct correlation with the analyzed variable, which can be seen in the example graph (Figure 4 for $F_{f_{RMS}}$ and Figure 5. for $F_{fN_{RMS}}$). These graphs show a test of force correlation in feed direction, normal feed direction and tool wear. It was decided to use multiple regression (4) to check whether the combination of all variables into one

equation, i.e. taking into account the impact of a given variable while taking into account the impact of other variables, would improve the quality of prediction. Analysis of the impact of individual parameters is important due to the elimination of the possibility of simple dependencies.

$$VB_c = 0.17v_c - 0.68a_p - 0.66a_e - 0.28v_f + 1.37F_{f_{RMS}} - 0.58F_{f_{p-p}} - 0.51F_{fN_{RMS}} - 0.29F_{fN_{ripple}} + 0.25F_{fN_{p-p}} - 0.2F_{z_{RMS}} + 0.91F_{z_{ripple}} - 0.04F_{z_{p-p}} + 0.42t_c + 0.1 \quad (4)$$

As assumed, the correlation coefficient R^2 increased, but its value was still very low and amounted to 0.4. Figure 6 shows the correlation of predictions for multiple regression.

The dispersion of the results is so large that the effectiveness of tool monitoring based on regression models is unsatisfactory. The prediction system must therefore be based on more advanced algorithms, such as ANN.

The research resulted in 230 cases for which the previously described measures were determined. Longer measurement sections were divided into several parts. In the first part of the research, the most effective activation functions were determined. The best effects of the network showed the use of the tanh function (5) as the activation in the hidden layer and the logistic function (6) as the activation of the output layer. All subsequent networks are based on the same functions and the BFGS (Broyden-Fletcher-Goldfarb-Shanno) learning algorithm. The advantages of this algorithm are low sensitivity to input data errors and low sensitivity to line search errors. The learning set was 70% of input data, the validation set was 15% and the testing set was 15% of all input data. The variables were randomly assigned to the sets. ANNs were selected choosing the highest coefficient R^2 and the lowest possible root mean square error (RSME) for testing data set. Maximum number of epochs (iterations) needed to complete the learning of ANN equal 200, that is the moment when the variability of weights for given network is less than or equal to 0.0001.

$$\tanh = \frac{e^x - e^{-x}}{e^x + e^{-x}} \quad (5)$$

$$\text{logistic} = \frac{1}{1 + e^{-x}} \quad (6)$$

The first set of networks was built using all cutting parameters and measures. Figure 7 shows a diagram of such a neural network.

Table 3. Full data of passes

nr	tool nr	t_c [min]	VB_c [mm]	v_c [m/min]	v_f [mm/min]	a_e [mm]	a_p [mm]
1	1	0.27	0.015	30	111	0.1	6
2	1	0.47	0.032	30	152	0.5	1
3	1	0.75	0.034	25	108	0.3	3.5
4	1	1.14	0.037	25	76	0.3	3.5
5	1	1.42	0.037	25	107	0.75	3.5
6	1	1.70	0.043	35	108	0.75	3.5
7	1	1.90	0.043	35	152	0.3	3.5
8	1	2.17	0.045	35	111	0.3	3.5
9	1	2.44	0.047	30	111	0.5	6
10	1	2.71	0.048	30	111	1	6
11	1	3.10	0.059	35	76	0.75	9
12	1	3.30	0.060	25	152	0.3	9
13	1	3.57	0.060	35	111	0.3	3.5
14	1	3.77	0.062	30	152	0.5	12
15	1	3.96	0.064	35	152	0.75	3.5
16	1	4.16	0.068	35	152	0.75	3.5
17	1	4.36	0.075	30	152	0.5	6
18	1	4.64	0.078	40	107	0.5	6
19	1	4.92	0.080	25	107	0.75	9
20	1	5.19	0.083	35	111	0.75	3.5
21	1	5.73	0.083	35	55	0.75	3.5
22	1	5.94	0.085	35	148	0.3	3.5
23	1	6.13	0.088	35	152	0.75	3.5
24	1	6.41	0.088	30	108	0.5	1
25	1	6.69	0.090	40	107	0.5	6
26	1	7.09	0.090	30	76	0.5	1
27	1	7.36	0.093	30	111	0.5	6
28	1	7.63	0.093	25	111	0.3	9
29	1	7.83	0.095	35	152	0.3	3.5
30	1	8.02	0.095	35	152	0.3	9
31	1	8.30	0.098	25	107	0.3	9
32	1	8.57	0.100	35	111	0.75	9
33	1	8.78	0.103	35	148	0.3	9
34	1	9.05	0.105	30	111	0.5	12
35	1	9.32	0.105	15	108	0.5	6
36	1	9.60	0.110	35	107	0.3	3.5
37	1	9.80	0.113	35	152	0.75	9
38	2	0.41	0.061	30	73	0.5	6
39	2	0.61	0.061	35	152	0.3	9
40	2	0.89	0.067	25	108	0.75	9
41	2	1.08	0.067	35	152	0.75	3.5
42	2	1.35	0.071	30	111	0.5	6
43	2	1.63	0.085	35	107	0.75	3.5
44	2	1.84	0.085	30	149	0.5	6
45	2	2.23	0.093	25	76	0.3	3.5
46	2	2.64	0.093	30	73	0.5	6
47	2	2.92	0.095	25	108	0.75	3.5

48	2	3.19	0.098	30	111	0.5	6
49	2	3.39	0.100	30	149	0.5	6
50	2	3.80	0.100	30	73	0.5	6
51	2	4.00	0.100	35	152	0.3	9
52	2	4.39	0.105	25	76	0.3	3.5
53	2	4.67	0.105	25	108	0.75	3.5
54	2	4.95	0.110	35	107	0.75	9
55	2	5.35	0.110	25	76	0.3	9
56	2	5.62	0.110	25	108	0.3	3.5
57	2	5.62	0.118	25	76	0.75	9
58	2	5.89	0.120	30	111	0.5	1
59	2	6.17	0.120	25	108	0.3	3.5
60	2	6.44	0.123	30	111	0.5	1
61	2	6.72	0.130	35	107	0.3	3.5
62	3	0.39	0.015	25	76	3.5	0.75
63	3	0.94	0.035	40	55	6	0.5
64	3	1.14	0.040	15	148	6	0.5
65	3	1.54	0.053	25	76	9	0.3
66	3	1.82	0.059	35	108	9	0.3
67	3	2.09	0.060	25	108	9	0.75
68	3	2.37	0.060	25	107	3.5	0.3
69	3	2.65	0.062	25	107	3.5	0.3
70	3	3.05	0.073	35	76	3.5	0.3
71	3	3.33	0.075	35	107	3.5	0.3
72	3	3.53	0.080	25	152	3.5	0.75
73	3	3.80	0.085	25	111	3.5	0.75
74	3	4.19	0.088	30	76	6	0.1
75	3	4.46	0.088	30	111	6	0.5
76	3	5.01	0.088	30	55	6	1
77	3	5.21	0.090	35	149	9	0.3
78	3	5.49	0.093	25	108	9	0.75
79	3	5.88	0.095	35	76	9	0.75
80	3	6.16	0.098	30	108	12	0.5
81	3	6.55	0.098	25	76	3.5	0.3
82	3	6.82	0.098	25	111	3.5	0.3
83	3	7.10	0.098	25	108	3.5	0.75
84	3	7.50	0.100	25	76	3.5	0.75
85	3	7.78	0.100	30	107	6	0.5
86	3	8.05	0.100	15	111	6	0.5
87	3	8.44	0.103	30	76	6	1
88	3	8.72	0.108	25	107	9	0.3
89	3	9.12	0.118	35	76	9	0.75
90	3	9.39	0.120	25	111	9	0.75

Then, the average global sensitivity of the network to variables was analyzed (Figure 8). Sensitivity analysis gives insight into the usefulness of individual input variables. It indicates variables that can be omitted without losing network

quality and key variables that must never be omitted. The measurement of network sensitivity is the quotient of the error obtained at the start of the network for the data set without one variable and the error obtained with the set of variables.

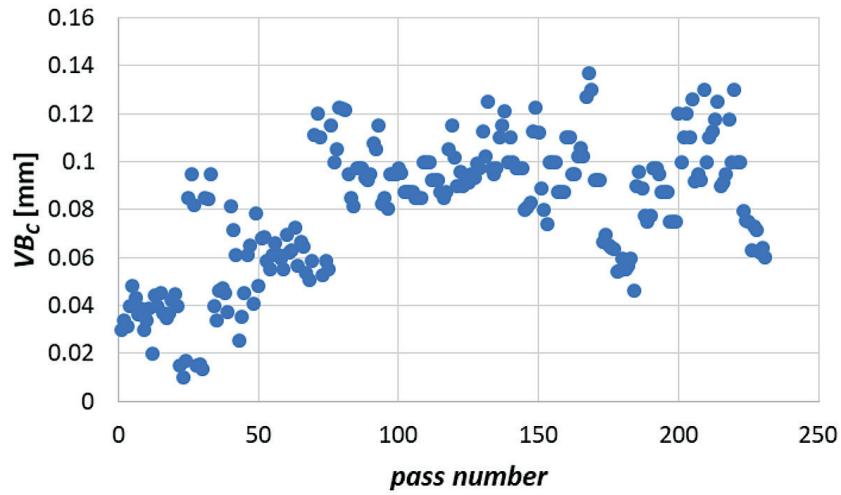


Figure 3. All tool wear results

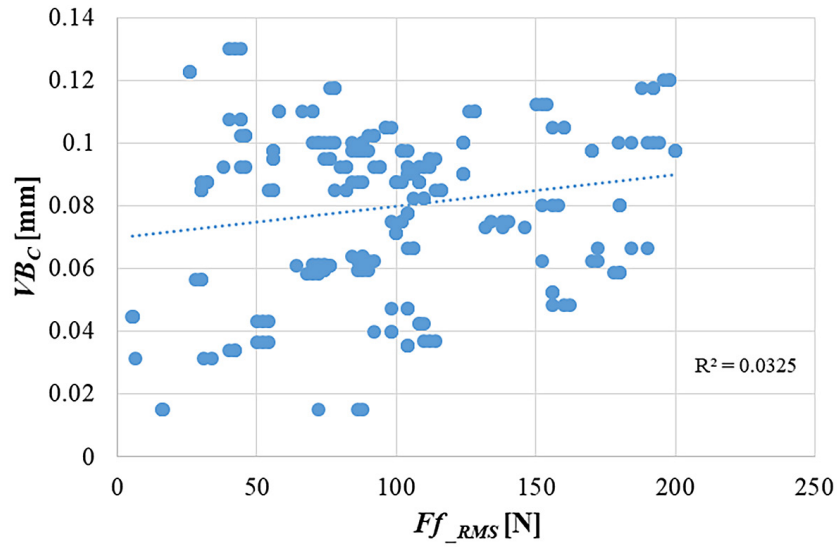


Figure 4. Relationship between force in feed direction Ff_{RMS} and tool wear VB_c

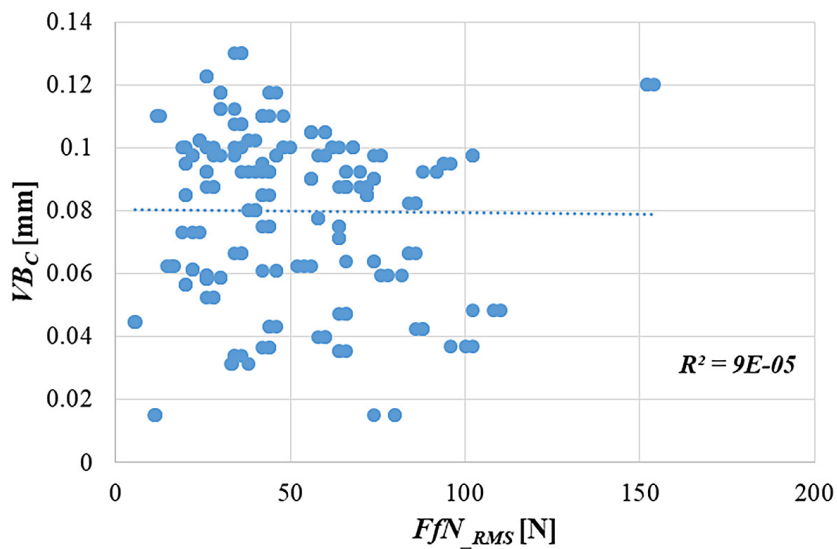


Figure 5. Relationship between force in feed direction FfN_{RMS} and tool wear VB_c

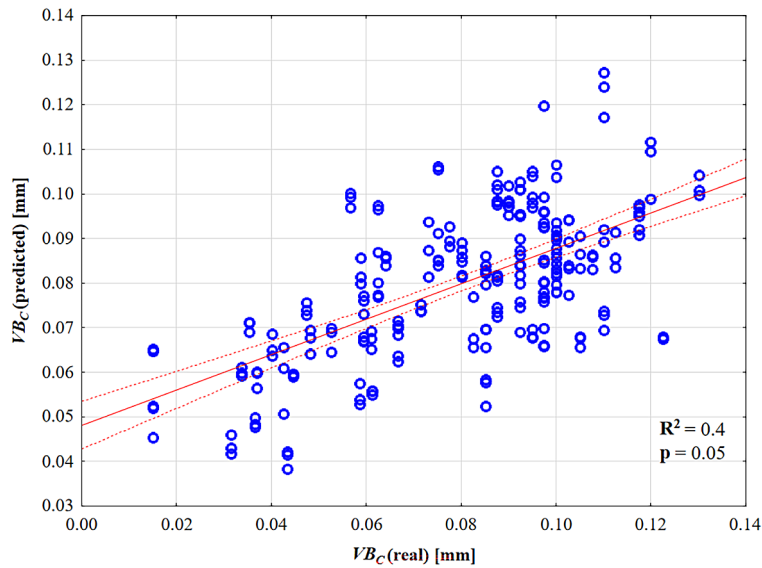


Figure 6. Correlation of predicted and measured variables for multiple regression

The greater the error after rejecting the variable is, in relation to the original error, the more sensitive the network is to the absence of this variable. For easier interpretation of the data, the sensitivity was normalized and presented in the graphs in this form.

On this basis, it was possible to eliminate two independent variables with the least impact on the prediction error from the training set. A comparison of the quality of the best networks can be found in Table 4.

As the built models do not show a satisfactory prediction quality, in the next step it was decided to supplement the learning set with the cutting time, and to re-analyze the sensitivity of the network (Figure 9). Previously rejected variables

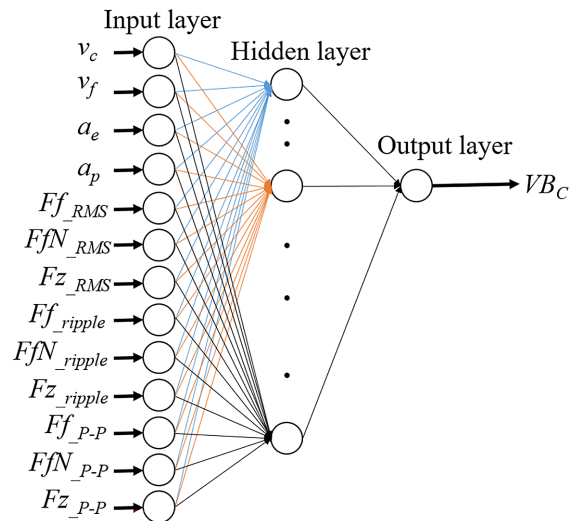


Figure 7. Scheme of a neural network

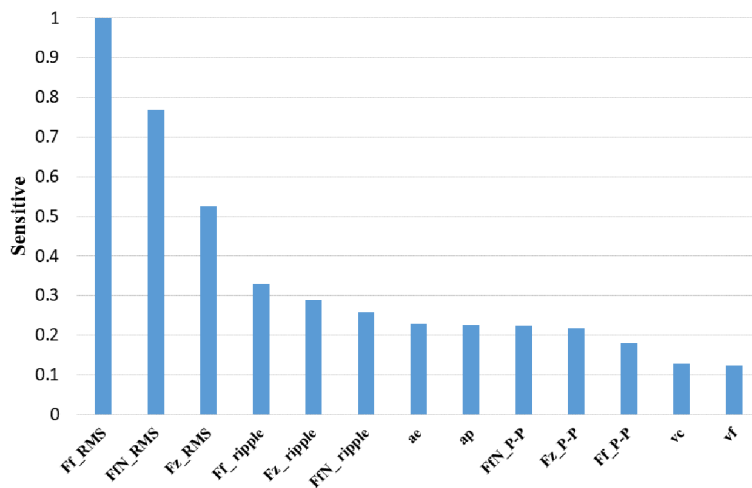


Figure 8. Normalized sensitivity of the network to input variables

Table 4. Network quality with all variables (MLP 13-15-1) and without v_f and v_c (MLP 11-10-1)

ANN structure	Learning quality	Validation quality	Testing quality
MLP 13-15-1	0.97	0.82	0.89
MLP 11-10-1	0.92	0.81	0.85

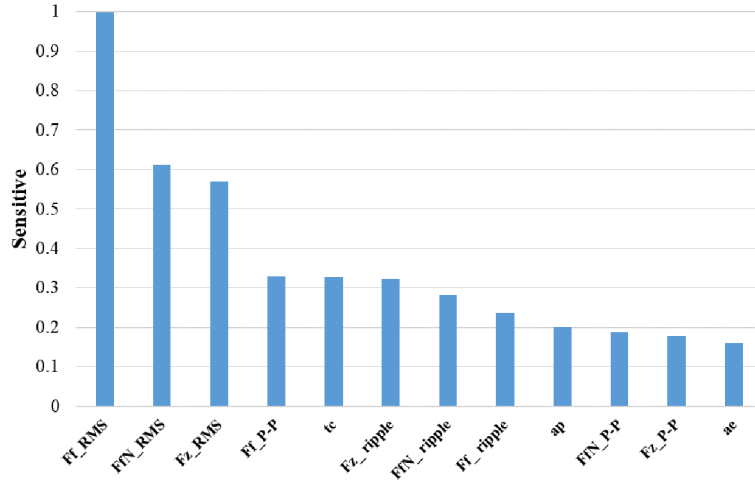


Figure 9. Normalized sensitivity of the network to variables taking into account the cutting time t_c

were not taken into account in the built models. Based on the sensitivity results (Figure 9), the data was reselected, rejecting those whose sensitivity did not exceed 0.2. In this way, all cutting

parameters and peak-to-peak values in the z-direction and in the normal feed direction were removed from the input data set. A comparison of the quality of the webs taking into account the

Table 5. Quality of neural networks including cutting time with all variables (MLP 12-10-1) and with a limited set of input variables (MLP 8-7-1)

ANN structure	Learning quality	Validation quality	Testing quality
MLP 12-10-1	0.99	0.95	0.95
MLP 8-7-1	0.95	0.94	0.94

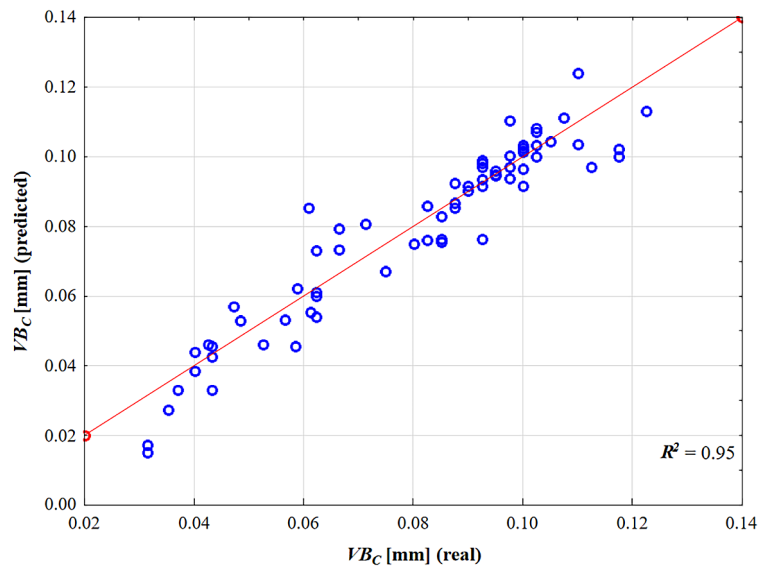


Figure 10. Correlation of predicted and measured variables for the MLP 12-10-1 network

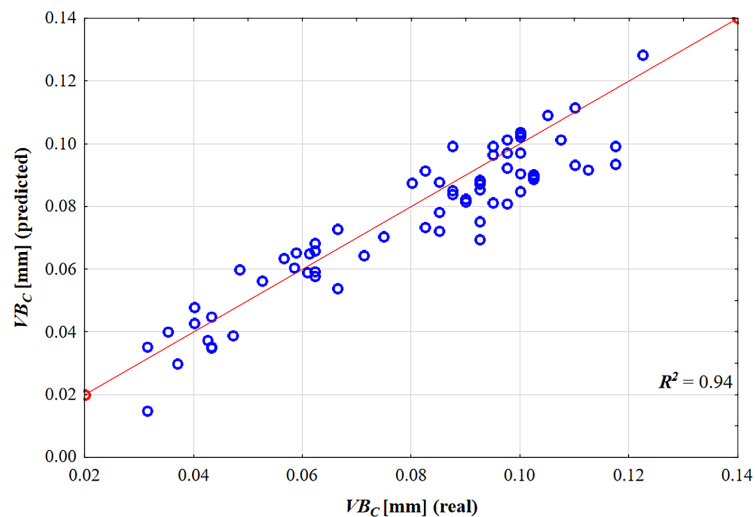


Figure 11. Correlation of predicted and measured variables for the MLP 8-7-1 network

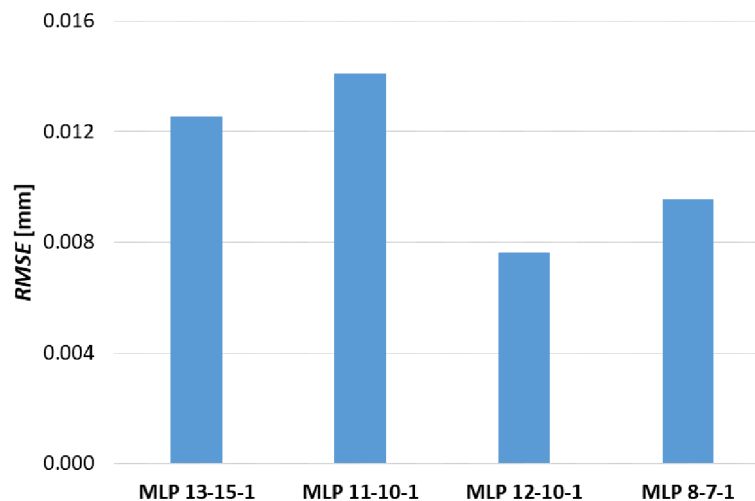


Figure 12. Comparison of the RMSE error for the best networks for a given set of training variables

cutting time is presented in Table 5. As can be seen, the removal of subsequent variables did not significantly worsen the quality of the network, but resulted in its clear simplification. The input data in the final prediction model comes only from the measurement of forces and easily measurable cutting time, but does not require entering data on cutting parameters. The graphs below show graphical correlations between predicted and actual variables measured for the MLP 12-10-1 network (Figure 10) and the MLP 8-7-1 network (Figure 11) for the data from the validation and testing sets. In the final step, the $_RMSE$ errors for all networks presented above are summarized in the graph (Figure 12).

The obtained RMSE errors for networks with cutting time are lower than the measurement accuracy of the workshop microscope used, which

was 0.01 mm. It can be noticed that the addition of the cutting time to the set of learning variables resulted in a decrease in the RMSE prediction error almost twice compared to networks not containing this variable, while further reduction of the learning set causes a slight increase in the error with a significant simplification of the system construction.

CONCLUSIONS

Based on the research and carried out analysis, the following conclusions can be formulated:
 1. In the examined range of cutting parameters, the use of single-variable regression and multiple regression equations is not an effective method of predicting the value of tool wear. It

shows little correlation for multiple regression ($R^2 = 0.4$) and no correlation for one variable.

2. In the case of artificial neural networks, a much better prediction quality was obtained, especially for models with a cutting time of MLP 12-10-1 and MLP 8-7-1 ($R^2 > 0.9$). It is important that to predict the value of the tool wear parameter, it is not necessary to enter the value of any of the cutting parameters. The absence of these variables in the set of input variables did not result in a significant increase in the prediction error. The error for the network containing the MLP 12-10-1 width and depth of cut was $RMSE = 0.0076$ mm, while the error for the network without cutting parameters was $RMSE = 0.0096$ mm.
3. Changing the cutting parameters causes a change in the level of cutting forces, usually greater than in the case of wear, so the cutting parameters do not have to be entered into the model. This change results from the change in the cross-section of the cutting layer.
4. The most important diagnostic measures turned out to be the RMS values of forces in all directions, especially in the feed direction ($F_{f_{RMS}}$). The RMS values, by averaging the values, reflect the variability of the forces than the peak to peak values, the increase of which would reveal tool damage if it occurred during machining.
5. The applied model allows for the derivation of the tool wear control track based on the force sensor, what is important, the cutting parameters can be variable during tool operation, which is common when using the tool in industry, and this will not cause significant errors in the wear indication.

REFERENCES

1. Wojciechowski, S.; Przystacki, D.; Chwalczuk, T. The evaluation of surface integrity during machining of Inconel 718 with various laser assistance strategies. *MATEC Web of Conference* 2017; 136, 01006-1–01006-6.
2. Zhou, J.; Bushlya, V.; Peng, R.L.; Johansson, S.; Stahl, J.E. Analysis of subsurface microstructure and residual stresses in machined Inconel 718 with PCBN and Al₂O₃-SiCw tools. *Procedia CIRP* 2014; 13, 150–155.
3. Xavier, M.A.; Manohar, M.; Madhukar, P.M.; Jeyapandiarajan, P. Experimental investigation of work hardening, residual stress and microstructure during machining Inconel 718. *J. of Mechanical Science and Technology* 2017; 31(10), 4789–4794.
4. Ren, X.-P.; Liu, Z.-Q. Microstructure refinement and work hardening in a machined surface layer induced by turning Inconel 718 super alloy. *Int. J. of Minerals, Metallurgy and Materials* 2018; 25(8), 937–949.
5. Liao, Y.S.; Lin, H.M.; Wang, J.H. Behaviors of end milling Inconel 718 superalloy by cemented carbide tools. *J. of Materials Processing Technology* 2008; 201(3–1), 460–465.
6. Musfirah, A.H.; Ghani, J.A.; Haron, C.H.C. Tool wear and surface integrity of inconel 718 in dry and cryogenic coolant at high cutting speed. *Wear* 2017; 376–377, 125–133.
7. Li, W.; Guo, Y.B.; Barkey, M.E.; Jordon, J.B. Effect tool wear during end milling on the surface integrity and fatigue life of inconel 718. *Procedia CIRP* 2014; 14, 546–551.
8. Mrkvica, I.; Špalek, F.; Szotkowski, T. Influence of cutting tool wear when milling Inconel 718 on resulting roughness. *Manufacturing Technology* 2018; 18(3), 457–461.
9. Drouillet, C.; Karandikar, J., Nath, C.; El Mansori, M.; Kurfess, T. Tool life predictions in milling using spindle power with the neural network technique. *J. of Manufacturing Processes* 2016; 22, 161–168.
10. Twardowski P.; M. Wiciak-Pikula M. Prediction of tool wear using artificial neural networks during turning of hardened steel. *Materials* 2019; 12(19), 3091-1–3091-15.
11. Liu, M.; Yao, X.; Zhang, J.; Jing, X.; Wang, K. Multi-sensor data fusion for remaining useful life prediction of machining tools by iabc-bpnn in dry milling operations. *Sensors* 2020; 20(17), 4657, 1–24.
12. Lu, X.; Jia, Z., Wang, H.; Wang, X.; Jia. Surface roughness prediction model of micro-milling Inconel 718 with consideration of tool wear. *Int. J. of Nanomanufacturing* 2016; 12(1), 93–108.
13. Khorasani, A.M.; Yazdi, M.R.S. Development of a dynamic surface roughness monitoring system based on artificial neural networks (ANN) in milling operation. *Int. J. of Advanced Manufacturing Technology* 2017; 93(1–4), 141–151.
14. Prasad, M.V.R.D.; Sravya, Y.; Tejaswi, K.S. Study of the influence of process parameters on surface roughness when Inconel 718 is dry turned using CBNCutting tool by artificial neural network approach. *Int. J. of Mat., Mech. and Manuf.* 2014; 2(4), 335–338.
15. D’Addona, D.; Segreto, T.; Simeone, A.; Teti, R. ANN tool wear modelling in the machining of nickel superalloy industrial products. *CIRP Journal of Manufacturing Science and Technology* 2011; 4(1), 33–37.
16. Leone, C.; D’Addona, D.; Teti, R. Tool wear modelling through regression analysis and intelligent

- methods for nickel base alloy machining. *CIRP Journal of Manufacturing Science and Technology* 2011; 4(3), 327–331.
17. Kalra, G.; Gupta, A.K. Mathematical modeling to estimate machining time during milling of Inconel 718 workpiece using ANN. *Materials Today: Proceedings* 2023; 78, 546–554.
 18. Sen, B.; Mia, M.; Mandal, U.K.; Mondal, S.P. GEP- and ANN-based tool wear monitoring: a virtually sensing predictive platform for MQL-assisted milling of Inconel 690. *International Journal of Advanced Manufacturing Technology* 2019; 105(1–4), 395–410.
 19. Kaya, B.; Oysu, C.; Ertunc, H.M. Force-torque based on-line tool wear estimation system for CNC milling of Inconel 718 using neural networks. *Advances in Engineering Software* 2011; 42(3), 76–84.
 20. Bagga, P.J.; Chavda, B.; Modi, V.; Makhesana, M.A.; Patel, K.M. Indirect tool wear measurement and prediction using multi-sensor data fusion and neural network during machining. *Materials Today: Proceedings* 2022; 51–55.
 21. Han, C.; Kim, K.B.; Lee, S.W.; Jun, M.B.-G.; Jeong, Y.H. *International Journal of Precision Engineering and Manufacturing* 2021; 22(9), 1527–1536.